JOURNAL OF NANO- AND ELECTRONIC PHYSICS
Vol. **5** No 4, 04055(6pp) (2013)

ЖУРНАЛ НАНО- ТА ЕЛЕКТРОННОЇ ФІЗИКИ
Том **5** № 4, 04055(6cc) (2013)

Effect of Substrates Types on CO Gas Sensing of SnO_2 Thin Film Prepared by Sol-Gel Method

Sumanta Kumar Tripathy[1,*], Bhabani Prasad Hota[2], V. Siva Jahnavy[3]

[1] *GVP College of Engineering (Autonomous), Madhurawada, Visakhapatanam, A.P., India*
[2] *Godavaris Mahavidyalaya, Banpur, Khurda, Odisha, India*
[3] *GVP College of Engineering for Women, Visakhapatanam, A.P., India*

(Received 18 July 2013; in final form 28 January 2014; published online 31 January 2014)

Tin oxide thin film was synthesized on glass and quartz substrate by sol-gel dip coating process taking tin (II) chloride as precursor and methanol as solvent. XRD study confirmed the tetragonal rutile structure of SnO_2. It was concluded that the transmission was higher and grain size was bigger in case of quartz than glass substrate from the study of optical characteristics by UV/VIS Spectrophotometer and SEM micrographs. CO gas sensing property of SnO_2 thin film was studied and it was revealed that the sensitivity of SnO_2 thin film grown on quartz substrate shows better performance than the film grown on glass substrate under the same conditions. Sensitivity of the film to CO gas was measured at different temperatures and was found to be highly sensitive at 220 °C for glass substrate and 210 °C for quartz substrate, at 50 ppm concentration. The result of change in conductivity of the sensors in presence of CO gas was also reported.

Keywords: Dip coating, Diffractometer, FWHM, Spectrophotometer, XRD.

PACS numbers: 68.37 Hk, 68.55. – a, 78.40. – q, 78.66. – w.

1. INTRODUCTION

In present days environmental pollution is a great concern among the researchers due to exhaust of combustible and process gases mostly from industry and motor vehicles. It is very important to protect the environment from those pollutant gases. To control and safely monitor the pollutant gases different methods like gas chromatography, FTIR spectroscopy, semiconductor gas sensors etc. have been adopted by the researchers. Solid state semiconducting gas sensors have substantial compensation than the other gas detection techniques. Generally semiconducting transparent materials with high transmittance, high band gap, resistant to high temperature and mechanically hard are used for gas sensors. Semiconducting sensors are reliable, easy to miniaturize, less costly, easy to produce and can be designed to operate over a wide range of conditions. Due to vibrant advancement of nanotechnology, especially on thin film technology, it has become relatively easy to synthesize semiconducting gas sensors. Semiconducting gas sensors, also called as chemo-resistive gas sensors, are typically based on metal oxides. The rehabilitated interest of researchers in SnO_2 which is based on metal oxide is due to its properties such as reflectivity, transparency, low electrical sheet resistance etc. Tin oxide crystallizes in tetragonal rutile structure with unit cell parameters, which are $a = b = 4.737$ Å and $c = 3.186$ Å. It is a n-type semiconductor having high band gap energy (≈ 3.6 eV) [1]. It is more transparent in the region of visible spectrum due to high band gap, having high electrical conductivity due to free electrons in oxygen vacancy holes. It is also hard and chemically stable due to which tin oxide thin films are of greater significance for the researchers. Due to above properties, tin oxide thin films are not only used extensively for gas-sensing and gas monitoring devices [2-3], but also in transistors [4], protective and wear-resistant coating on glass containers [5], photovoltaic cell [6], transparent conductive electrode for solar cells [7], photochemical and photoconductive devices in liquid crystal display [8] etc.

The current paper describes the preparation and study of sensing characteristics of tin oxide (SnO_2) grown on both glass and quartz substrates. According to stoichiometry, tin oxide is an insulator at room temperature. But when thin film of tin oxide comes in contact with air, the surface of film absorbs oxygen [9] at grain boundaries which ensnared electrons and build a barrier around each grain [10], which behaves like doping, and produces ionization levels close to the bottom of the conduction band and finally exhibits the property of n-type semiconductor. The gas sensing properties of tin oxide thin films have been performed for different gases like CO, NO_x, H_2S, H_2, CH_4 and CNG etc.[11-13]. Till today so many methods were adopted to synthesize doped or un-doped tin oxide films such as thermal evaporation [14-15], chemical vapor deposition [16-17], R.F. magnetron Co-sputtering [18], laser pulse evaporation [19-20], spray pyrolysis [21-24] and sol-gel [25-27]. Among these techniques, sol-gel method play an important role due to several advantages such as simple experimental arrangement, easy control on film thickness with a high porosity area which can improve the efficiency of the sensors, less processing cost, greater homogeneity and more purity. In this study we espoused dip coating method. Starting from tin(II) chloride which is preferred due to low cost as precursor, methanol as solvent and glacial acetic acid as chelating agent, transparent solution was prepared and SnO_2 thin film was synthesized on a glass substrate and quartz by sol-gel dip coating technique. Our main intention in this work

* sktripathy2009@gmail.com

was to prepare SnO_2 thin films by sol-gel method on glass and quartz substrates and to investigate the influence of the nature of the substrate on the optical, morphological and CO gas sensing properties.

Structural analysis of the films was carried out by XRD measurement using SIEMENS Diffractometer (Model D5000). The study confirms tetragonal rutile structure of SnO_2 and the preferential growth along direction (101). The optical properties were studied by the equipment ELICO UV / VIS spectrophotometer (Model – SL-159) in the wavelength range from 300 nm to 1000 nm. The transmission graph showed that for nearly same thickness and under the same conditions the transmission was higher in case of quartz than glass substrates and also band gap was less in case of quartz substrate. Surface morphology was examined from SEM micrographs by using Scanning Electron microscope (Model- Philips XL 30). Using both XRD and SEM it was observed that the grain size and strain of SnO_2 thin film are larger in the case of quartz substrate than glass substrate. Sensitivity analysis was done with the help of homemade equipment [28] and it was revealed that the sensitivity of SnO_2 thin film grown on quartz substrate is more than the film grown on glass substrate at concentration 50 ppm.

2. EXPERIMENTAL DETAILS

2.1 Preparation of Solution

1 gm of anhydrous tin (II) chloride ($SnCl_2$) is dissolved in 50 ml of methanol (CH_3OH) with 1 gm glacial acetic acid (CH_3COOH) and stirred by a stirrer for 45 minutes at NTP to get a clear and homogeneous solution. The glass and quartz substrates were thoroughly cleaned with cleaning liquid soap and then with acetone to remove organic particles on the surface and then washed with distilled water. The substrates were then soaked with TEA diluted isopropyle alcohol for 10 minutes and then dried to prevent local hydrolysis.

2.2 Preparation of Film

Then the substrates were dipped in the prepared solution by hand and withdrawn. The coated substrates were dried at 150 °C in a muffler furnace for 1 hr and then heat treated at 300 °C for about 15 minutes. The above procedure was repeated for a number of times to get the desired thickness. We repeated the procedure for six times to get a thickness of 645-650 nm in this study. After getting the required thickness the final heat treatment was carried for each substrate at 500 °C for one and half hour in the muffler furnace in air.

2.3 Gas Sensing Description

The change of electrical properties of the metal-oxide semiconductor due to adsorb gas molecules is responsible for SnO_2 sensor response which is due to surface interactions between tin oxide and the surrounding gases. The steps involved in sensor response to exposure to air and to a reducing gas, were described below. When thin film of SnO_2 was exposed to air, oxygen from the air is adsorbed onto the surface of the SnO_2 thin film. Electrons from the surface region of the SnO_2 are transferred to adsorbed oxygen, leading to the formation of an electron-depleted region near the surface of SnO_2 film. The electron depleted region, where electron density is less, is an area of high resistance and the core region of the film, where electron densities are high, is an area of relatively low resistance. Now the adsorbed oxygen becomes O^- and O_2^- species. When the thin film of SnO_2 is exposed to a reducing gas like CO, surface reactions such as $CO + O_{ads}^- \rightarrow CO_2 + e^-$ and $2CO + O_{2,ads}^- \rightarrow 2CO_2 + 2e^-$ took place. Due to which electrons release and the electrons released from surface reaction transfer back into the conduction band leading to decrease in the resistance or increase in conductance of SnO_2 thin film.

Sensitivity test was carried out in a closed chamber containing heating element. Just above the heating element a polished iron slab (sample holder) with a thermocouple was placed. The sample was placed on the sample holder. Two conducting probes were placed on the sample at extreme ends of the film to measure the resistance at different temperatures. Before putting the sample on the sample holder it was heated to 300 °C for 30 minutes to remove water vapor and then cooled to room temperature. Then resistance of the sample was measured with the help of Precision LCZ meter at different temperatures of the sample. Carbon monoxide gas concentration of about 50 ppm was injected to the chamber for measurement of resistance in presence of CO gas at different temperatures.

3. RESULTS AND ANALYSIS

3.1 Optical Measurement

Optical characterization was studied from transmission % vs. wavelength curve which was plotted from the data obtained from transmission spectrum analysis of the film by ELICO UV/VIS spectrophotometer Model- SL-159 in the wavelength range from 300 nm to 1000 nm. The refractive index and the thickness of the film were calculated using the formula [29-30].

$$n = \left\{ \left(2\mu \frac{T_u - T_l}{T_u T_l} + \frac{\mu^2 + 1}{2} \right) + \left(\left(2\mu \frac{T_u - T_l}{T_u T_l} + \frac{\mu^2 + 1}{2} \right)^2 - \mu^2 \right)^{1/2} \right\}^{1/2}$$

and $d = \left| \frac{\lambda_1 \lambda_2}{4(n_1 \lambda_2 - n_2 \lambda_1)} \right|$

Where 'n' and 'd' are the refractive index and thickness of the thin film 'μ' refractive index of the substrate; T_u and T_l are the transmission maximum at upper envelop and transmission minimum at lower envelop for a particular wavelength λ; n_1 and n_2 are the refractive index of the thin film at maxima (for wave length λ_1) and corresponding minima (for wave length λ_2) where phase difference is π.

The transmission % vs. wavelength curve was plotted from the data obtained from transmission spectrum and is shown in fig. 1. From fig. 1 it is clear that the transmission of SnO_2 thin film is very high in the visible region of the spectra, due to the fact that the reflec-

tivity is low and there is less absorption due to excitation of electrons from the valence band to conduction band. Fig. 1 also depicts the excellent surface quality and homogeneity of the thin film which substantiates the semiconducting properties of the film as it was established by Nowak[31], that the pure semiconducting compounds have sharp absorption edge.

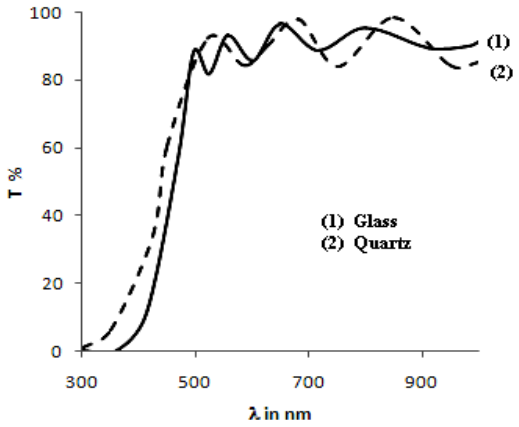

Fig. 1 – T % vs. λ in mm in the wavelength range 300 -1000 nm

From fig. 1 it is obvious that transmittance is higher in case of quartz substrate than glass substrate. It may be due to high porosity and larger grain size and less absorption in the film deposited on quartz substrate than glass substrate. It is also clear that transmission values are more than 0.80 at wave length greater than 450 nm in both cases. From the transmission Vs. wavelength graph average refractive index and thickness were calculated as 2.07 and 2.13 are for glass and quartz substrates respectively. The smaller value of refractive index for glass substrate may be probably due to the increase of homogenity and surface smoothness of the films due to smaller grain size in the case of glass substrate.

From the transmission graph in the UV region the absorption coefficient (α) can be calculated from the expression [32] $\alpha = d^{-1}\ln(T^{-1})$, where '$d$' is thickness of the film and 'T' is optical transmission. The calculated absorption co-efficient was about 10^4 cm^{-1} for both the cases. The band gap [33] was calculated from the graph $(\alpha h\upsilon)^{1/2}$ vs. $h\upsilon$ in SnO_2 thin film deposited on quartz and glass substrates. It has been observed that the band gap was 3.7 eV and 3.62 eV in case of SnO_2 thin film deposited on glass and quartz substrates respectively. This band gap value suitably matches the values given by J.E. Dominquez [34]. The smaller band gap of the film deposited on quartz substrate may be due to improvement of the degree of crystallization and growth of grain.

3.2 Structural and Morphological Analysis

The structure of the film was investigated by XRD which was carried out by Siemens Diffractometer Model D-5000 using CuKα having wavelength $\lambda = 0.1540$ nm radiation with diffraction angle from 10° to 70°. XRD spectra of SnO_2 thin film deposited on quartz and glass substrates using the above described technique are shown in fig. 2.

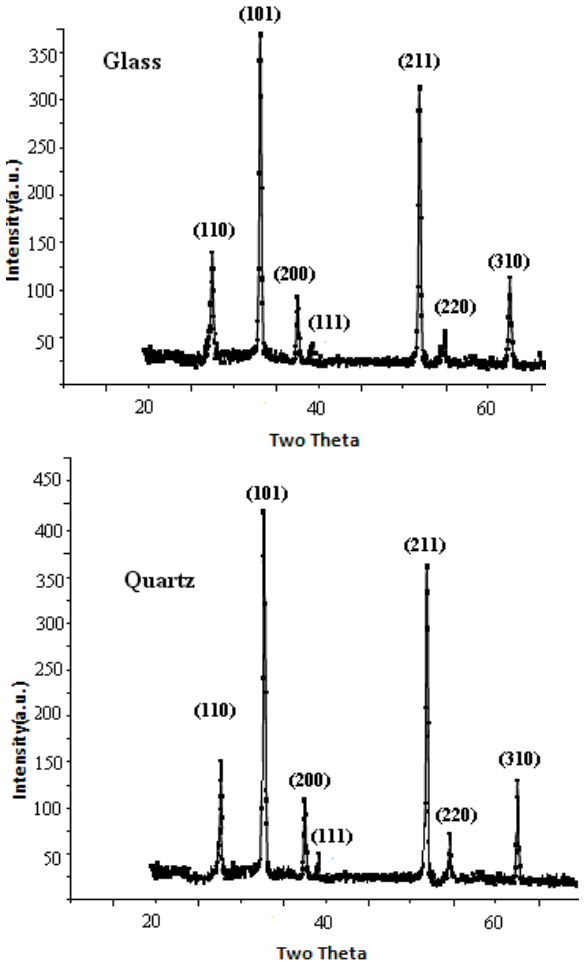

Fig. 2 – XRD Pattern of SnO_2 thin film deposited on glass and quartz substrates

Fig. 2 clearly depicts well defined very narrow and sharp diffraction peaks which show higher crystalline quality of SnO_2 film and are appropriately matched to JCPDS Card No. 88-0287 which shows the crystalline tetragonal rutile structure of SnO_2. The well defined peaks which match the standard interplanar spacing was given as 26.6° for (110) plane, 33.9° for (101) plane, 38° for (200) plane, 39° for (111) plane, 51.8° for (211) plane, 54.8° for (220) plane and 61.9° for (310) plane. The (101) peak has the largest intensity in both the cases, but others (101), (110), (200), (220) and (310) are also clearly detected. Since the intensity of (101) plane was higher it may be believed that the preferential growth along direction (101) hence Sn forms an interstitial bond with oxygen and exist as rutile SnO_2. There is a marked increase in the intensity of the X-ray diffraction peaks in case of quartz substrate than as observed in the glass substrate which may be due to additional nucleation centers for SnO_2.

Grain size of the film was calculated by using Debye-Scherrer formula and the average grain size of the deposited film was calculated as 48.54 and 51.27 nm for the film grown on glass and quartz substrates. This difference may be probably due to the presence of more strains in the film grown on quart substrate.

Morphological study was conceived out from the SEM images of SnO_2 thin film deposited on glass and

quartz substrates which were shown in fig. 3. SEM micrographs show agglomeration of the grain particles in both cases, but explicitly more in case of quartz substrate. The SEM images clearly depict changes in microstructure and in grain size under the same conditions. SEM micrograph of thin film made a conclusion that the grain size is little bigger in case of quartz substrate due to the bigger size of domes in case of quartz substrate.

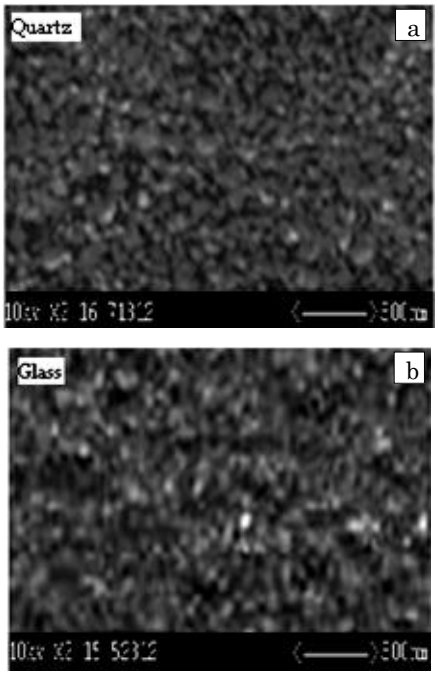

Fig. 3 – SEM images of SnO_2 film for quartz and glass substrates

The grain size estimated from SEM images was 50.12 nm and 52.45 nm for glass and quartz substrates respectively. The result is a little bigger than the grain size determined by Debye-Scherrer formula.

3.3 Sensitivity Analysis

The gas sensing reactions are due to surface sensitivity. The increase in surface area due to nanosize of the film increases the probability of the reaction and hence the sensitivity. The sensitivity of SnO_2 gas sensor is typically defined as the ratio of the surface resistance (R_a) of the film in air to that in the target gas (R_g) i.e. Sensitivity = R_a/R_g, when thin film surface of SnO_2 was exposed to air, due to adsorbance, electron depletion layer is formed where electron density is less and thus a layer of high resistance is formed and the adsorb oxygen remains in the form of O^- and O_2^- species. So the high resistance of SnO_2 thin film is present in air. When the thin film surface of SnO_2 was exposed to CO reducing gas due to surface reaction more e^- were released. These released electrons transfer back in to the conduction band which increases the conductivity or decreases the resistance of SnO_2 film. The sensitivity of SnO_2 thin film for carbon monoxide gas was studied at concentration 50 ppm. The variation of the sensitivity with temperature is shown in fig. 7.

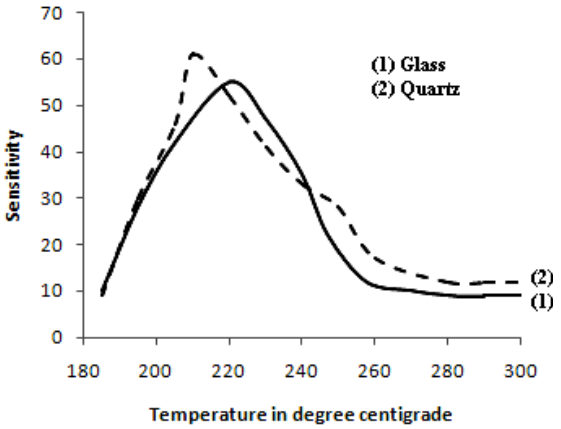

Fig. 4 – Sensitivity vs. temperature in °C

Fig. 4 shows clearly that maximum sensitivity occurs at temperature of 220 °C for glass substrate and 210 °C for quartz substrate. At low temperatures there is less oxygen coverage, when the sensor is exposed to air and therefore when the target gases are introduced there is negligible change in sensitivity. As the operating temperature increases, the number of adsorbed oxygen species would react more and more electrons which are released due to this reaction are sent back to conduction band i.e. the desorption rate of adsorbed gases also increases with increasing of temperatures. As temperature increases further, more adsorbed oxygen species react and more electrons are sent back to conduction band leading to increase in conductivity. At 220 °C, which is known as critical temperature T_c, almost all adsorb oxygen species react and maximum electrons are sent back to conduction band leading to maximum sensitivity. The decrease in sensitivity for temperatures above the critical operating temperature, T_c, can be attributed to the higher desorption rates at these temperatures. When the target gases are introduced, the added desorption due to the target gases is relatively small for the steady-state desorption in air, leading to decreasing impact on the sensor response for $T > T_c$. Due to the competing rates of adsorption and desorption, tin oxide sensors always tend to exhibit maximum sensitivity at the particular operating temperature, called critical temperature. The critical temperature for the film grown on quartz substrate is

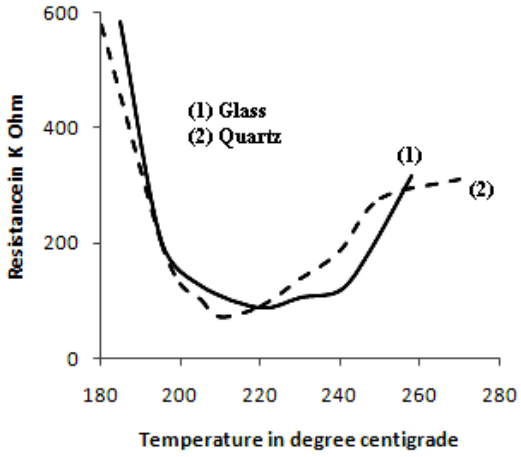

Fig. 5 – Resistance vs temperature in CO gas

less than the critical temperature for the film grown on glass substrate. The higher sensitivity of SnO_2 film grown on quartz substrate for CO gas may be probably due to greater adsorption of oxygen molecules.

The graph which shows the relation between resistance of SnO_2 film in the presence of CO gas and temperature is shown in fig. 5. It depicts that at low temperature less number of adsorbed oxygen species undergo desorption and less number of electrons which are released due to this, are sent back to conduction band resulting in high resistance of the film surface. As temperature increases, more adsorbed oxygen undergo desorption resulting in more electron in conduction band which leads to less resistance of the thin film. At critical temperature (220 °C for glass substrate and 210 °C for quartz substrate) almost all adsorbed oxygen reacts and maximum number of electrons are sent back to conduction band resulting in minimum resistance of the thin film. Above the critical temperature the resistance of the film increases which may be due to the fact that the added desorption due to the target gases is relatively small for the steady-state desorption in air.

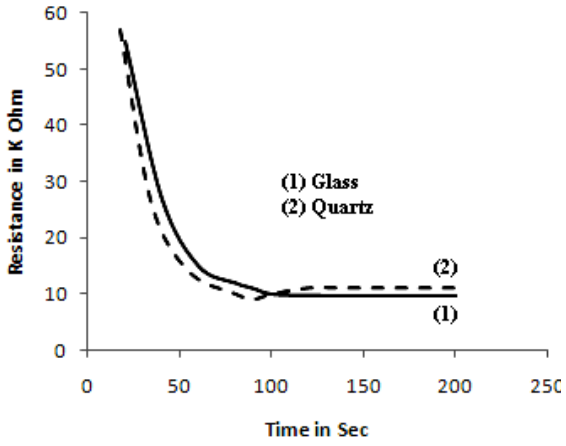

Fig. 6 – Resistance vs time in CO gas

The variation of resistance with time i.e. the response time of the thin films is shown in fig. 9. The response time graph was plotted at 220 °C for glass substrate and 210 °C for quartz substrate. Figure clear shows that there is a rapid decrease in resistance of about 45 K Ohms (in case of glass substrate) and of about 48 K Ohms (in case of quartz substrate) in nearly 100 second after injection of CO gas at 50 ppm, which clearly indicates that the rate of desorption is a little higher in case of SnO_2 film grown on quartz substrate than glass substrate.

Fig. 6 concludes that the response time is 20 sec (for glass substrate) and 18 sec (for quartz substrate) and saturation resistance of the film is achieved after nearly 100 sec in both cases which may be due to the fact that after 100 sec there will be no adsorb oxygen species left for desorption.

4. CONCLUSION

Semiconducting tin oxide thin film was synthesized on glass substrate by sol-gel dip coating method. The thickness of the film was calculated as 645.98 nm using optical measurement. XRD study revealed the grain size as 48.5 nm and the product was of tetragonal rutile structure. From SEM images it was concluded that the surface roughness of the film in case of quartz substrate is higher. EDS result confirms the purity of SnO_2 thin film. The film was studied for carbon monoxide gas sensing. It was observed that the sensitivity of the film was higher at 220 °C in case of glass substrate and 210 °C in case of quartz substrate using CO gas at concentration 50ppm. The study of response time analysis concluded that the response time was very high i.e. 20 sec in case of glass substrate at 220 °C and 18 sec in case of quartz substrate at 210 °C using carbon monoxide gas at concentration 50 ppm. The given time is generally very short for gas sensing applications. Finally it was concluded that semiconductor metal oxide gas sensing thin film may be grown on the quartz substrate for better performance.

ACKNOWLEDGEMENT

Authors are grateful to Prof. T.S.N. Somayaji, Director, Centre for Nano Science and Technology, GVP College of Engineering (Autonomous) for providing laboratory facilities and his incessant support to expedite the investigation work.

REFERENCES

1. C. Kilic, A. Zunger, *Phys. Rev. Lett.* **88**, 095501(2002).
2. A. Keshavraja, A.V. Ramaswami, K. Vijayamohanan, *Sensor. Actuat. B* **23**, 75 (1995).
3. N. Butta, L. Cinquegrani, E. Mugno, A. Tagliente, S. Pizzini, *Sensor. Actuat. B: Chem.* **6**, 253(1992).
4. M.S.Arnold, P.Avouris, Z.W.Pan, and Z.L.Wang, *J. Phys. Chem. B: Chem.* **107**, 659(2003).
5. M. Nakagawa, T. Amano S. Yokokura, *J. Non-Cryst. Solids* **218**, 100 (1997).
6. H. Cachet, J. Bruneaux, G. Folcher, C. Levy-Clement, C. Vard, M. Neumann-Spallart, *Sol. Energ. Mater. Sol. C.* **46**, 101 (1997).
7. A. Mohammadi-Gheidari, E. Soleimani Asl, M. Mansorhoseini, S. Mohajerzadeh, N. Madani, W. Shams-Kolahi, *Mater. Res. Bull.* **40**, 1303 (2005).
8. U. Betz, Kharrazi, M. Olsson, J. Marthy, M.F. Escola, F. Atamny, *Surf. Coat. Technol.* **200**, 5751 (2006).
9. K. Ihokura, J. Watson, *The Stannic Oxide Gas Sensors: Principles and Applications* (CRC Press: London: 1994).
10. V.R. Katti, A.K. Debnath, K.P. Muthe, M. Kaur, A.K. Dua, S.C. Gadkari, S.K. Gupta, V.C. Sahni, *Sensor. Actuat. B: Chem.* **96**, 245 (2003).
11. R.S. Niranjan, I.S. Mulla, *Mater. Sci. Eng. B* **103**, 103 (2003).
12. O.K. Varghase, L.K. Malhotra, *Sensor. Actuat. B: Chem.* **53**, 19 (1998).
13. N.S. Baik, G. Sakai, N. Miura, N. Tamajoe, *Sensor. Actuat. B: Chem.* **63**, 74 (2000).
14. E. Comini, G. Faglia, G. Sberveglieri, Z. Pon, Z.L. Wang, *Appl. Phys. Lett.* **81**, 1869 (2002).
15. V.S. Vaishnav, P.D. Patel, N.G. Patel, *Thin Solid Films* **490**, 94 (2005).

16. P.M. Gorley, V.V. Khomyak, S.V. Bilichuk, I.G. Orletsky, P.P. Hovly, V.O. Grechko *Mater. Sci. Eng. B* **118**, 160 (2005).
17. R.Jr. Mamazza, D.L. Morel, C.S. Ferekider, *Thin Solid Films* **484**, 26 (2005).
18. K.S. Yoo, S.H. Park, J.H. Karg, *Sensor. Actuat. B: Chem.* **108**, 159 (2005).
19. H.T. Yang, J.T. Cheung, *J. Cryst. Growth*, **56**, 429 (1982).
20. H. Fang, T.M. Miller, R.H. Magruder, R.A. Weller, *J. Appl. Phys.* **91**, 6194 (2002).
21. H. Pirmoradi, J. Malakootikhah, M. Karimipour, A. Ahmadpour, N. Shahtahmasebi, F.E. Koshky, *Middle-East Journal of Scientific Research* **8** No 1, 253 (2011).
22. D.W. Lane, J.A. Coath, K.D. Rogers, B.J. Hunnikin, H.S. Beldon, *Thin Solid Films* **221**, 262 (1992).
23. F. Paraguay, D.W. Estrada, L.D.R. Acosta, N.E. Andradeb, M. Miki-Yoshida, *Thin Solid Films* **350**, 192 (1999).
24. G. Blandenet, M. Court, Y. Lagarde, *Thin Solid Films* **77**, 81 (1981).
25. O. Culha, M.F. Ebeoglugil, I. Birlik, E. Celik, M. Toparli, *J. Sol-Gel Sci. Technol.* **51**, 32 (2009).
26. J.P. Chatelon, C. Terrier, E. Bemstein, R. Berjoan, J.A. Roger, *Thin Solid Films* **247**, 162 (1994).
27. B. Orel, U. Lavrenčič-Štankgar, Crnjak-Orel, P. Bukovec, M. Kosec, *J. Non-Cryst. Solids* **167**, 272 (1994).
28. S. Mishra, C. Ghanshyam, N. Ram, S. Singh, R.P. Bajpai, R.K. Bedi, *Bull. Mater. Sci.* **25** No 3, 231 (2002).
29. J.C. Manifacier, J. Gasiot, J.P. Fillard, *J. Phys. E: Sci. Instrum.* **9**, 1002 (1976).
30. S.K. Tripathy, P.V. Rajeswari, B.P. Hota, *Bull. Mater. Sci.* **35**, (2002) (in Press)
31. M. Nowak, *Thin Solid Films* **266**, 258 (1995).
32. R.D. Tarey, T.A. Raju, *Thin Solid Films* **128**, 181 (1985).
33. K.D. Girase, *J. Nano-Electron. Phys.* **5**, 03013 (2013)
34. J.E. Dominquez, X.Q. Pan, L. Fu, P.A. Vanrompay, Z. Zhang, J.A. Nees, P.P. Pronko, *J. Appl. Phys.* **91**, 1060 (2002).